

Article

Ammoniates of Zintl Phases: Similarities and Differences of Binary Phases A_4E_4 and Their Corresponding Solvates

Corinna Lorenz , Stefanie Gärtner and Nikolaus Korber * 

Institute of Inorganic Chemistry, University of Regensburg, 93055 Regensburg, Germany; Corinna.Lorenz@ur.de (C.L.); Stefanie.Gaertner@ur.de (S.G.)

* Correspondence: Nikolaus.Korber@ur.de; Tel: +49-941-943-4448; Fax: +49-941-943-1812

Received: 20 April 2018; Accepted: 23 June 2018; Published: 29 June 2018



Abstract: The combination of electropositive alkali metals A (A = Na-Cs) and group 14 elements E (E = Si-Pb) in a stoichiometric ratio of 1:1 in solid state reactions results in the formation of polyanionic salts, which belong to a class of intermetallics for which the term Zintl compounds is used. Crystal structure analysis of these intermetallic phases proved the presence of tetrahedral tetrelide tetraanions $[E_4]^{4-}$ precast in solid state, and coulombic interactions account for the formation of a dense, three-dimensional cation-anion network. In addition, it has been shown that $[E_4]^{4-}$ polyanions are also present in solutions of liquid ammonia prepared via different synthetic routes. From these solutions crystallize ammoniates of the alkali metal tetrahydrides, which contain ammonia molecules of crystallization, and which can be characterized by X-ray crystallography despite their low thermal stability. The question to be answered is about the structural relations between the analogous compounds in solid state vs. solvate structures, which all include the tetrahedral $[E_4]^{4-}$ anions. We here investigate the similarities and differences regarding the coordination spheres of these anions and the resulting cation-anion network. The reported solvates $Na_4Sn_4 \cdot 13NH_3$, $Rb_4Sn_4 \cdot 2NH_3$, $Cs_4Sn_4 \cdot 2NH_3$, $Rb_4Pb_4 \cdot 2NH_3$ as well as the up to now unpublished crystal structures of the new compounds $Cs_4Si_4 \cdot 7NH_3$, $Cs_4Ge_4 \cdot 9NH_3$, $[Li(NH_3)_4]_4Sn_4 \cdot 4NH_3$, $Na_4Sn_4 \cdot 11.5NH_3$ and $Cs_4Pb_4 \cdot 5NH_3$ are considered for comparisons. Additionally, the influence of the presence of another anion on the overall crystal structure is discussed by using the example of a hydroxide co-crystal which was observed in the new compound $K_{4.5}Sn_4(OH)_{0.5} \cdot 1.75 NH_3$.

Keywords: Zintl compounds; liquid ammonia; crystal structure

1. Introduction

The term “polar intermetallics” applies to a large field of intermetallic compounds, the properties of which range from metallic and superconducting to semiconducting with a real band gap [1–5]. For the compounds showing a real band gap, the Zintl–Klemm concept is applicable by formally transferring the valence electrons of the electropositive element to the electronegative partner, and the resulting salt-like structure allows for the discussion of anionic substructures [1–9]. The combination of electropositive alkali metals A (A = Na-Cs) and group 14 elements E (E = Si-Pb) in a stoichiometric ratio of 1:1 in solid state reactions results in the formation of salt-like, semiconducting intermetallic compounds which show the presence of the tetrahedral $[E_4]^{4-}$ anions precast in solid state. These anions are valence isoelectronic to white phosphorus and can be seen as molecular units. They have been known since the work of Marsh and Shoemaker in 1953 who first reported on the crystal structure of NaPb [10]. Subsequently, the list of the related binary phases of alkali metal and group 14 elements was completed (Table 1, Figure 1). Due to coulombic interactions a dense,

three-dimensional cation-anion network in either the KGe structure type (A = K-Cs; E = Si, Ge) [11–17] or NaPb structure type (A = Na-Cs; E = Sn, Pb) (Figure 1e,f) [18–21] is observed. For sodium and the lighter group 14 elements silicon and germanium, binary compounds lower in symmetry (NaSi: $C2/c$ [14,16,17,22], NaGe: $P2_1/c$ [14,16]) are formed, which also contain the tetrahedral shaped $[E_4]^{4-}$ anions (Figure 1c,d). In the case of lithium, no binary compound with isolated $[E_4]^{4-}$ polyanions is reported at ambient conditions: In LiSi [23] and LiGe [24] (LiSi structure type, Figure 1a), threefold bound silicon atoms are observed in a three-dimensionally extended network, which for tetrel atoms with a charge of -1 is an expected topological alternative to tetrahedral molecular units, and which conforms to the Zintl–Klemm concept. If the $[E_4]^{4-}$ cages are viewed as approximately spherical, the calculated radius r would be 3.58 Å for silicide, 3.67 Å for germanide, 3.96 Å for stannide and 3.90 Å for plumbide clusters (r = averaged distances of the center of the cages to the vertex atoms + van der Waals radii of the elements, each [25]). The dimensions for silicon and germanium are very similar, as are those for tin and lead. It is worth noticing that there is a significant increase in the size of the tetrahedra, which are considered as spherical, for the transition from germanium to tin, which could explain the change of the structure type KGe to NaPb.

For binary compounds of lithium and tin or lead, the case is different. The Zintl rule is not applicable as LiSn (Figure 1b) [26] includes one-dimensional chains of tin atoms, whereas NaSn [19,27] forms two-dimensional layers as the tin substructure. For LiPb [28] the CsCl structure has been reported, which is up to now unreproduced.

Table 1. Binary phases of alkali metal (Li-Cs) and group 14 element with 1:1 stoichiometric ratio (ambient conditions).

	Si	Ge	Sn	Pb
Li	$I4_1/a$ LiSi [23]	$I4_1/a$ LiSi [24]	$I4_1/amd$ [26]	CsCl (?) [28]
Na	$C2/c$ [14,16,17,22]	$P2_1/c$ [14,16]	$I4_1/acd$ NaPb [19,27]	$I4_1/acd$ NaPb [10]
K	$P-43n$ KGe [11,12,14]	$P-43n$ KGe [11,13]	$I4_1/acd$ NaPb [19,21]	$I4_1/acd$ NaPb [21]
Rb	$P-43n$ KGe [11,12,14]	$P-43n$ KGe [11,13,14]	$I4_1/acd$ NaPb [18,21]	$I4_1/acd$ NaPb [20,21]
Cs	$P-43n$ KGe [11,12,14]	$P-43n$ KGe [11,13,14]	$I4_1/acd$ NaPb [18,21]	$I4_1/acd$ NaPb [24]

Additionally, it has been shown that the tetrelide tetraanions are also present in solutions of liquid ammonia [29], and from these solutions alkali metal cation- $[E_4]^{4-}$ compounds that additionally contain ammonia molecules of crystallization can be precipitated. We earlier reported on the crystal structures of $Rb_4Sn_4 \cdot 2NH_3$, $Cs_4Sn_4 \cdot 2NH_3$ and $Rb_4Pb_4 \cdot 2NH_3$, which showed strong relations to the corresponding binaries [30]. In $Na_4Sn_4 \cdot 13 NH_3$ [31,32] no such relation is observed. In general, ammonia in solid ammoniates is not only an innocent and largely unconnected solvent molecule but may also act as a ligand towards the alkali metal cations. This leads to a variety of crystal structures, which allows for the investigation of the competing effects of cation-anion-interaction vs. alkali-metal-ammine complex formation in the solid state. We here report on the single crystal X-ray investigations of the new compounds $Cs_4Si_4 \cdot 7NH_3$, $Cs_4Ge_4 \cdot 9NH_3$, $[Li(NH_3)_4]_4Sn_4 \cdot 4NH_3$, $Na_4Sn_4 \cdot 11.5NH_3$ and $Cs_4Pb_4 \cdot 5NH_3$ and compare the previously reported solvates as well as the new ammoniate compounds of tetratetrelide tetraanions to the known binary compounds. It has to be noted that the number of ammoniate structures of tetrelide tetraanions is very limited [30–34] as they are easily oxidized in solution by forming less reduced species like $[E_9]^{4-}$ [35–40] and $[E_5]^{2-}$ [36,41–43]. In Table 2, all hitherto known ammoniates which contain the highly charged $[E_4]^{4-}$ (E = Si-Pb) cluster are listed. For $[Sn_9]^{4-}$ we could recently show that co-crystallization of hydroxide anions is possible in the compound $Cs_5Sn_9(OH) \cdot 4NH_3$ [44]. We here present the first crystal structure of the co-crystal of $[Sn_4]^{4-}$ and the hydroxide anion in the compound $K_{4.5}Sn_4(OH)_{0.5} \cdot 1.75 NH_3$ which allows for the discussion of the influence of another anion on the overall crystal structure.

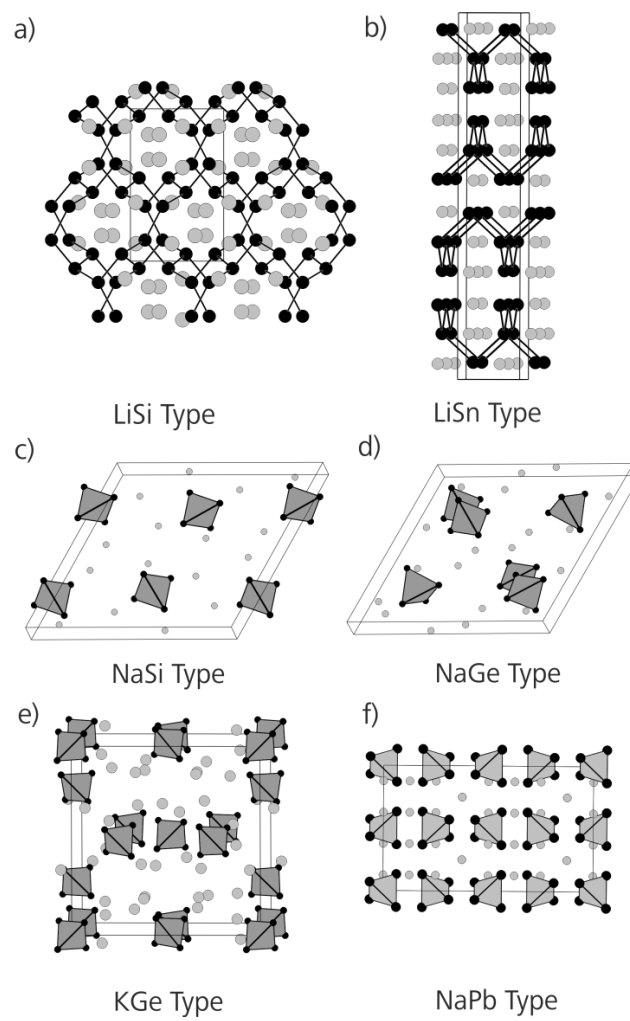


Figure 1. Different structure types for the binary phases of alkali metal (Li-Cs) and group 14 element with 1:1 stoichiometric ratio (ambient conditions) (a–f).

Table 2. Hitherto known $A_4E_4 \cdot xNH_3$ ($A = Li-Cs$; $E = Si-Pb$) solvate structures and selected crystal structure details. The bold marked new compounds are discussed in this article.

	Compound	Crystal System	Space Group	Unit Cell Dimensions
Si	Cs₄Si₄·7NH₃	triclinic	<i>P</i> -1	a = 12.3117(6) Å; b = 13.0731(7) Å; c = 13.5149(7) Å; V = 2035.88(19) Å ³
Ge	Cs₄Ge₄·9NH₃	orthorhombic	<i>Ibam</i>	a = 11.295(2) Å; b = 11.6429(15) Å; c = 17.237(2) Å; V = 2266.9(6) Å ³
Sn	[Li(NH ₃) ₄] ₄ Sn ₄ ·4NH ₃	monoclinic	<i>I</i> 2/ <i>a</i>	a = 16.272(3) Å; b = 10.590(2) Å; c = 20.699(4) Å; V = 3446.9(13) Å ³
	[Li(NH ₃) ₄] ₉ Li ₃ (Sn ₄) ₃ ·11NH ₃ [31]	monoclinic	<i>P</i> 2/ <i>n</i>	a = 12.4308(7) Å; b = 9.3539(4) Å; c = 37.502(2) Å; V = 4360.4(4) Å ³
	Na₄Sn₄·11.5NH₃	monoclinic	<i>P</i> 2 ₁ / <i>c</i>	a = 13.100(3) Å; b = 31.393(6) Å; c = 12.367(3) Å; V = 5085.8(18) Å ³
	Na ₄ Sn ₄ ·13NH ₃ [31,32]	hexagonal	<i>P</i> 6 ₃ / <i>m</i>	a = b = 10.5623(4) Å; c = 29.6365(16) Å; V = 2863.35 Å ³
	K ₄ Sn ₄ ·8NH ₃ [31]	hexagonal	<i>P</i> 6 ₃	a = b = 13.1209(4) Å; c = 39.285(2) Å; V = 5857.1(4) Å ³
	Rb ₄ Sn ₄ ·2NH ₃ [30]	monoclinic	<i>P</i> 2 ₁ / <i>a</i>	a = 13.097(4) Å; b = 9.335(2) Å; c = 13.237(4) Å; V = 1542.3(7) Å ³
	Cs ₄ Sn ₄ ·2NH ₃ [30]	monoclinic	<i>P</i> 2 ₁ / <i>a</i>	a = 13.669(2) Å; b = 9.627(1) Å; c = 13.852(2) Å; V = 1737.6(4) Å ³
Pb	Rb ₄ Pb ₄ ·2NH ₃ [30]	monoclinic	<i>P</i> 2 ₁ / <i>a</i>	a = 13.170(3) Å; b = 9.490(2) Å; c = 13.410(3) Å; V = 1595.2(6) Å ³
	Cs₄Pb₄·5NH₃	orthorhombic	<i>Pbcm</i>	a = 9.4149(3) Å; b = 27.1896(7) Å; c = 8.1435(2) Å; V = 2084.63(10) Å ³

2. Materials and Methods

For the preparation of $[E_4]^{4-}$ -containing solutions different preparative routes are possible which are described elsewhere [8]. In general, liquid ammonia was stored over sodium metal and was directly condensed on the reaction mixture under inert conditions (see Appendix A). The reaction vessels were stored for at least three months at 235 K or 197 K. For the handling of the very temperature and moisture labile crystals, a technique developed by Kottke and Stalke was used [45,46]. Crystals were isolated directly with a micro spatula from the reaction solutions in a recess of a glass slide containing perfluoroether oil, which was cooled by a steam of liquid nitrogen. By means of a stereo microscope, an appropriate crystal was selected and subsequently attached on a MicroLoop™ and placed on a goniometer head on the diffractometer. For details on the single crystal X-Ray structure analysis, please see Table 3.

Table 3. Crystal structure and structure refinement details for the compounds described above.

Chemical Formula	Cs ₄ Pb ₄ ·5NH ₃	Cs ₄ Ge ₄ ·9NH ₃	Cs ₄ Si ₄ ·7NH ₃	Na ₄ Sn ₄ ·11.5NH ₃	[Li(NH ₃) ₄] ₄ Sn ₄ ·4NH ₃	K _{4.5} Sn ₄ (OH) _{0.5} ·1.75NH ₃
CSD No. *	434173	434172	434176	421860	421857	427472
Mr [g·mol ⁻¹]	1445.57	948.09	763.24	1525.25	843.20	689.03
Crystal system	orthorhombic	orthorhombic	triclinic	monoclinic	monoclinic	monoclinic
Space group	<i>Pbcm</i>	<i>Ibam</i>	<i>P-1</i>	<i>P2₁/c</i>	<i>I2/a</i>	<i>P2₁/c</i>
<i>a</i> [Å]	9.4149(3)	11.295(2)	12.3117(6)	13.100(3)	16.272(3)	16.775(3)
<i>b</i> [Å]	27.1896(7)	11.6429(15)	13.0731(7)	31.393(6)	10.590(2)	13.712(3)
<i>c</i> [Å]	8.1435(2)	17.237(2)	13.5149(7)	12.367(3)	20.699(4)	26.038(5)
α [°]	90	90	85.067(4)	90	90	90
β [°]	90	90	73.052(4)	90.32(3)	104.90(3)	90.92(3)
γ [°]	90	90	78.183(4)	90	90	90
<i>V</i> [Å ³]	2084.63(10)	2266.9(6)	2035.88(19)	5085.8(18)	3446.9(13)	5988(2)
<i>Z</i>	4	4	4	4	4	16
<i>F</i> (000) (e)	2392.0	1644.0	1384.0	2800.0	1648.0	4920.0
ρ_{calc} [g·cm ⁻³]	4.606	2.778	2.490	1.968	1.625	3.057
μ [mm ⁻¹]	39.072	11.578	7.331	3.955	2.887	7.807
Absorption correction	numerical [47]	/	numerical [47]	numerical [48]	numerical [48]	numerical [48]
Diffractometer (radiation source)	Super Nova (Mo)	Super Nova (Mo)	Super Nova (Mo)	Stoe IPDS II (Mo)	Stoe IPDS II (Mo)	Stoe IPDS II (Mo)
2 θ - range for data collection [°]	6.24–52.74	6.9–48.626	6.3–50.146	3.892–51.078	4.072–50.91	3.836–50.966
Reflections collected/independent	18834/2274	2294/748	26514/7197	9587/9390	22976/3118	27272/10460
Data/restraints/parameters	2274/0/72	748/0/44	7197/30/377	9390/0/370	3118/9/163	10460/0/389
Goodness-of-fit on <i>F</i> ²	1.086	1.043	1.038	0.802	0.886	0.844
Final <i>R</i> indices [<i>I</i> > 2 σ (<i>I</i>)]	R1 = 0.0388, <i>wR</i> 2 = 0.0900	R1 = 0.0711, <i>wR</i> 2 = 0.1251	R1 = 0.0304, <i>wR</i> 2 = 0.0747	R1 = 0.0401, <i>wR</i> 2 = 0.1007	R1 = 0.0400, <i>wR</i> 2 = 0.0798	R1 = 0.0592, <i>wR</i> 2 = 0.1397
<i>R</i> indices (all data)	R1 = 0.0425, <i>wR</i> 2 = 0.0926	R1 = 0.1323, <i>wR</i> 2 = 0.1525	R1 = 0.0365, <i>wR</i> 2 = 0.0780	R1 = 0.0625, <i>wR</i> 2 = 0.1101	R1 = 0.0748, <i>wR</i> 2 = 0.0861	R1 = 0.1037, <i>wR</i> 2 = 0.1538
<i>R</i> _{int}	0.0884	0.1162	0.0343	0.1011	0.0965	0.0704
$\Delta\rho_{\text{max}}, \Delta\rho_{\text{min}}$ [e·Å ⁻³]	2.48/−2.32	1.70/−1.24	2.00/−2.22	1.90/−1.17	1.61/−0.62	3.86/−1.24

* Further details of the crystal structure investigations may be obtained from FIZ Karlsruhe, 76344 Eggenstein-Leopoldshafen, Germany (Fax: (+49)7247-808-666; e-mail: crysdata(at)fiz-karlsruhe(dot)de, on quoting the deposition numbers.

3. Results

In the following, the crystal structures of the new compounds $\text{Cs}_4\text{Pb}_4 \cdot 5\text{NH}_3$, $\text{Cs}_4\text{Ge}_4 \cdot 9\text{NH}_3$, $\text{Cs}_4\text{Si}_4 \cdot 7\text{NH}_3$, $\text{Na}_4\text{Sn}_4 \cdot 11.5\text{NH}_3$, $[\text{Li}(\text{NH}_3)_4]_4\text{Sn}_4 \cdot 4\text{NH}_3$ and $\text{K}_{4.5}\text{Sn}_4(\text{OH})_{0.5} \cdot 1.75\text{NH}_3$ are described independently, their similarities and differences towards the binary materials are discussed subsequently in Section 4 (Discussions).

3.1. $\text{Cs}_4\text{Pb}_4 \cdot 5\text{NH}_3$

The reaction of elemental lead with stoichiometric amounts of cesium in liquid ammonia yields shiny metallic, reddish needles of $\text{Cs}_4\text{Pb}_4 \cdot 5\text{NH}_3$. The asymmetric unit of the crystal structure of $\text{Cs}_4\text{Pb}_4 \cdot 5\text{NH}_3$ consists of three crystallographically independent lead atoms, four cesium cations and four ammonia molecules of crystallization. One of the lead atoms and one of the nitrogen atoms are located on the general *Wyckoff* position *8e* of the orthorhombic space group *Pbcm* (No. 57). The other two lead atoms, four Cs^+ cations and three nitrogen atoms occupy the special *Wyckoff* positions *4d* (mirror plane) and *4c* (twofold screw axis) with a site occupancy factor of 0.5 each. The Pb_4 cage is generated from the three lead atoms through symmetry operations. As there is no structural indication for the ammonia molecules to be deprotonated, the $[\text{Pb}_4]^{4-}$ cage is assigned a fourfold negative charge, which is compensated by the four cesium cations. The Pb-Pb distances within the cage range between 3.0523(7) Å and 3.0945(5) Å. They are very similar to those that have been found in the solventless binary structures (3.090(2) Å) [21]. The cluster has a nearly perfect tetrahedral shape with angles close to 60° . The tetraplumbide tetraanion is coordinated by twelve Cs^+ cations at distances between 3.9415(1)–5.4997(8) Å. They coordinate edges, faces and vertices of the cage (Figure 2e). The coordination sphere of Cs1 is built up by four $[\text{Pb}_4]^{4-}$ cages ($3 \times \eta^1$, $1 \times \eta^2$) and five ammonia molecules of crystallization. Here, the cesium cation is surrounded by four lead clusters tetrahedrally and thus forms a supertetrahedron (Figure 3a).

Cs2 and Cs4 are trigonally surrounded by three Pb_4 cages ($1 \times \eta^1$, $2 \times \eta^2$ and $2 \times \eta^1$, $1 \times \eta^3$) each. Their coordination spheres are completed by five and four ammonia molecules of crystallization, respectively, as shown for Cs2 in Figure 3b. Cs3 only shows contacts to two Pb_4 cages ($2 \times \eta^2$) and six ammonia molecules of crystallization (Figure 3c). Altogether, a two-dimensional network is formed. Along the crystallographic b-axis, corrugated Cs^+ - NH_3 strands are built. The $[\text{Pb}_4]^{4-}$ cages are situated along the strands and are stacked along the c-axis (Figure 4).

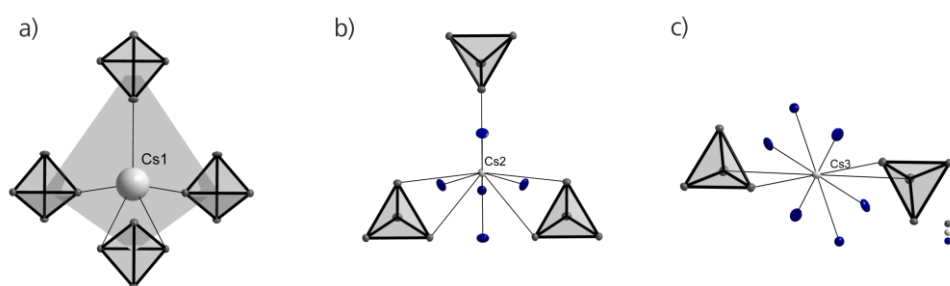


Figure 2. Comparison of the cationic coordination spheres of $[\text{E}_4]^{4-}$ ($\text{E} = \text{Sn}, \text{Pb}$) clusters in $\text{Na}_4\text{Sn}_4 \cdot 11.5\text{NH}_3$ (a); $\text{Rb}_4\text{Sn}_4 \cdot 2\text{NH}_3$ (b); NaPb (c); $\text{Rb}_4\text{Pb}_4 \cdot 2\text{NH}_3$ (d) and $\text{Cs}_4\text{Pb}_4 \cdot 5\text{NH}_3$ (e); probability factor: 50%; dark grey marked cations occupy special *Wyckoff* positions.

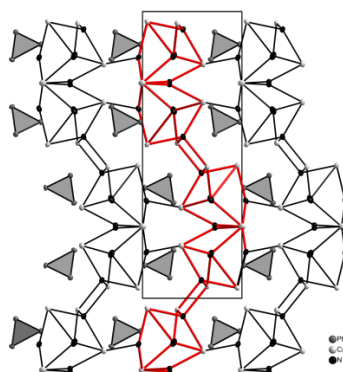


Figure 3. Coordination spheres of the cesium cations in $\text{Cs}_4\text{Pb}_4 \cdot 5\text{NH}_3$; (a) tetrahedral environment of Cs1 by $[\text{Pb}_4]^{4-}$, for reasons of clarity, ammonia molecules are omitted; (b,c) coordination spheres of Cs2 (representative for Cs4) and Cs3; for reasons of clarity, hydrogen atoms are omitted; probability factor: 50%.

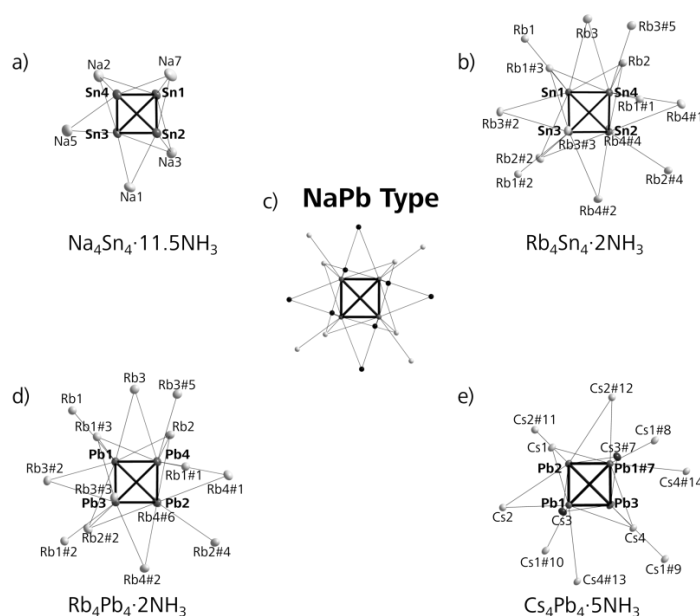


Figure 4. Section of the structure of $\text{Cs}_4\text{Pb}_4 \cdot 5\text{NH}_3$; corrugated $\text{Cs}^+ \cdot \text{NH}_3$ strands along the crystallographic b-axis; the chains are emphasized by bold lines; $[\text{Pb}_4]^{4-}$ cages are located along the strands; hydrogen atoms are omitted for clarity; probability factor: 79%.

3.2. $\text{Cs}_4\text{Ge}_4 \cdot 9\text{NH}_3$

Deep red needles of $\text{Cs}_4\text{Ge}_4 \cdot 9\text{NH}_3$ could be obtained by the dissolution of $\text{Cs}_{12}\text{Ge}_{17}$ together with two chelating agents, [18]crown-6 and [2.2.2]cryptand in liquid ammonia. Indexing of the collected reflections leads to the orthorhombic space group *Ibam* (No. 72). The asymmetric unit of this compound consists of one germanium atom, one cesium cation and four nitrogen atoms. The anionic part of the compound is represented by a $[\text{Ge}_4]^{4-}$ tetrahedron, which is generated by the germanium position through symmetry operations resulting in the point group D_2 for the molecular unit. The definite number of ammonia molecules of crystallization cannot be determined due to the incomplete data set (78%), but very likely sums up to four in the asymmetric unit. $\text{Cs}_4\text{Ge}_4 \cdot 9\text{NH}_3$ is the first ammoniate with a ligand-free tetragermanide tetraanion reported to date. In spite of the incomplete data set, the heavy atoms Cs and Ge could be unambiguously assigned as maxima in the Fourier difference map. The dimensions of the germanium cage (2.525(3)–2.592(3) Å) comply with the expected values found in

literature (2.59 Å [11]). The $[\text{Ge}_4]^{4-}$ anion shows almost perfect tetrahedral symmetry with Ge-Ge-Ge angles between $58.63(10)^\circ$ and $61.21(11)^\circ$. It is surrounded by eight cesium cations. They coordinate η^1 -like to edges and η^3 -like to triangular faces of the cage (Figure 5e). The coordination sphere of the cesium atom itself is built by two $[\text{Ge}_4]^{4-}$ cages and is completed by eight ammonia molecules of crystallization. Considering the Cs^+ - $[\text{Ge}_4]^{4-}$ contacts, layers parallel to the crystallographic a- and b-axis are formed, which are separated by ammonia molecules of crystallization.

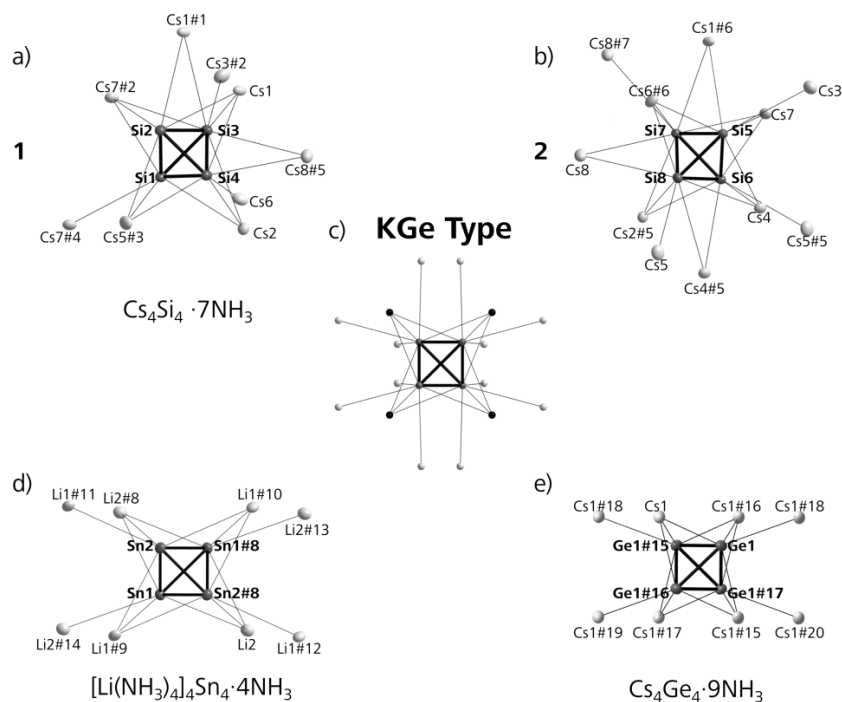


Figure 5. Comparison of the cationic coordination spheres of $[\text{E}_4]^{4-}$ ($\text{E} = \text{Si-Sn}$) clusters in $\text{Cs}_4\text{Si}_4 \cdot 7\text{NH}_3$ (a,b (two crystallographically independent $[\text{Si}_4]^{4-}$ cages)), KGe (c); $[\text{Li}(\text{NH}_3)_4]_4\text{Sn}_4 \cdot 4\text{NH}_3$ (d) and $\text{Cs}_4\text{Ge}_4 \cdot 9\text{NH}_3$ (e); probability factor: 50%; dark grey marked cations occupy special *Wyckoff* positions.

3.3. $\text{Cs}_4\text{Si}_4 \cdot 7\text{NH}_3$

Dissolving $\text{Cs}_{12}\text{Si}_{17}$ together with dicyclohexano[18]crown-6 and [2.2.2]cryptand in liquid ammonia resulted in deep red prismatic crystals of $\text{Cs}_4\text{Si}_4 \cdot 7\text{NH}_3$. The asymmetric unit consists of two crystallographically independent $[\text{Si}_4]^{4-}$ clusters, eight cesium cations and 14 ammonia molecules of crystallization. All atoms are located on the general *Wyckoff* position $2i$ of the triclinic space group $P-1$ (No. 2). $[\text{Si}_4]^{4-}$ (1) is surrounded by nine, $[\text{Si}_4]^{4-}$ (2) by eleven Cs^+ cations (Figure 5a,b). Here the cations span edges, faces and vertices of the clusters in a distance range of $3.559(2)$ – $4.651(3)$ Å. Cs1, Cs5, Cs7 and Cs8 are η^1 -, η^2 - and η^3 -like surrounded by three Si_4 cages each, which are arranged in a triangular shape (comparable to the coordination sphere shown in Figure 3b). The remaining four cesium cations per asymmetric unit also show ionic contacts to two silicon clusters each by spanning edges, faces and vertices of the latter. The coordination spheres of all alkali metal cations are completed by four to nine ammonia molecules of crystallization (Figure 6b). Altogether, a two-dimensional $[\text{Si}_4]^{4-}$ - Cs^+ -network is formed. The anionic cluster and the cations built corrugated waves, comparable to $\text{Cs}_4\text{Pb}_4 \cdot 5\text{NH}_3$ (Figure 4). The ammonia molecules of crystallization fill the space between the strands.

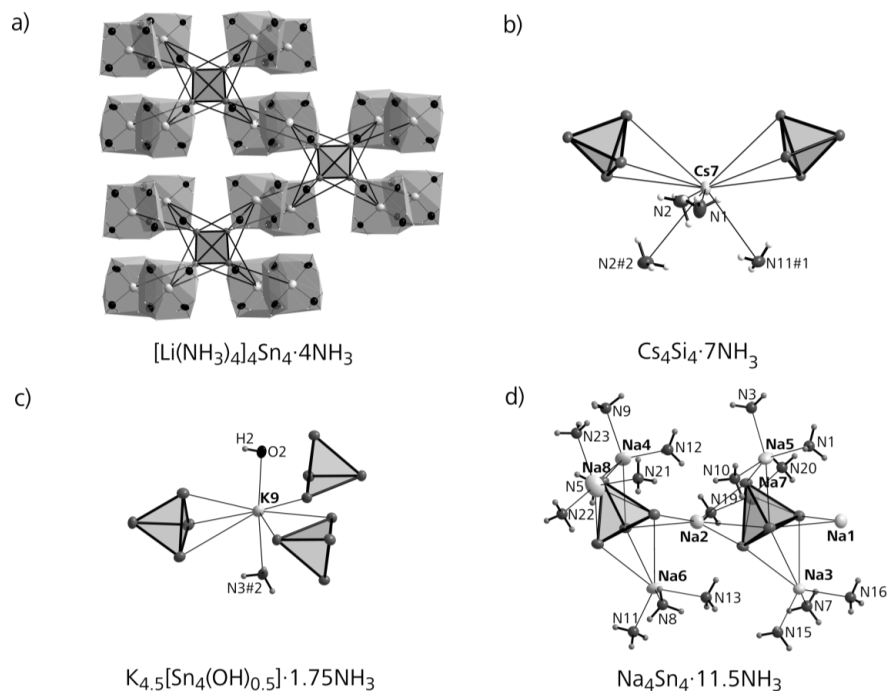


Figure 6. Coordination spheres of the cations; (a) $[\text{Li}(\text{NH}_3)_4]^+_4[\text{Sn}_4]^{4-}$ strands; for reasons of clarity, the $[\text{Li}(\text{NH}_3)_4]^+$ complexes are shown as spherical polyhedra; (b) of Cs7 in $\text{Cs}_4\text{Si}_4 \cdot 7\text{NH}_3$, representative for the coordination spheres of the heavier alkali metals; (c) of K9 in $\text{K}_{4.5}\text{Sn}_4(\text{OH})_{0.5} \cdot 1.75\text{NH}_3$ as a representative of the other cations in the structure; (d) complete coordination sphere of $[\text{Sn}_4]^{4-}$ anions and sodium cations; probability factor: 50%.

3.4. $\text{Na}_4\text{Sn}_4 \cdot 11.5\text{NH}_3$

Red, prism-shaped crystals of $\text{Na}_4\text{Sn}_4 \cdot 11.5\text{NH}_3$ could be synthesized by reacting elemental tin with stoichiometric amounts of sodium and $t\text{BuOH}$ in liquid ammonia. Two crystallographically independent $[\text{Sn}_4]^{4-}$ tetrahedra represent the anionic part of the asymmetric unit. The charge is compensated by eight sodium cations. Additionally, 23 ammonia molecules of crystallization can be found. All atoms occupy the general *Wyckoff* position $4e$ of the monoclinic space group $P2_1/c$ (No 14). Although the two $[\text{Sn}_4]^{4-}$ cages are crystallographically independent, the chemical environment is very similar (Figure 2a). Five sodium cations reside on edges and triangular faces of each cluster. Considering the anion-cation contacts, one-dimensional strands along the a -axis are formed. The tetrastannide clusters are bridged by two crystallographically independent sodium cations Na1 and Na2, which alternately coordinate faces and edges of the cages (Figure 6d). Thus the anionic part of the structure can be assigned the formula $1^\infty[\text{Na}(\text{Sn}_4)]^{3-}$. A similar coordination of the bridging atom was recently found in the ammoniate $\text{Rb}_6[(\eta^2\text{-Sn}_4)\text{Zn}(\eta^3\text{-Sn}_4)] \cdot 5\text{NH}_3$, where two $[\text{Sn}_4]^{4-}$ anions are bridged by a Zn^{2+} cation forming isolated dimeric units [49]. As already mentioned, Na1 and Na2 only show contacts to $[\text{Sn}_4]^{4-}$, the remaining six sodium cations additionally coordinate to ammonia molecules of crystallization. Altogether, a molecular formula of $[(\text{Sn}_4)\text{Na}]_2[(\text{Na}(\text{NH}_3)_3)_5(\text{Na}(\text{NH}_3)_2)] \cdot 6\text{NH}_3$ represents the whole crystal structure, where sodium- $[\text{Sn}_4]^{4-}$ strands are separated by both coordinating ammonia and unattached ammonia molecules of crystallization.

3.5. $[\text{Li}(\text{NH}_3)_4]_4\text{Sn}_4 \cdot 4\text{NH}_3$

The reaction of elemental tin with stoichiometric amounts of lithium and $t\text{BuOH}$ in liquid ammonia yields in black shaped crystals of $[\text{Li}(\text{NH}_3)_4]_4\text{Sn}_4 \cdot 4\text{NH}_3$. The asymmetric unit of the new compound consists of two tin atoms, two lithium atoms and ten ammonia molecules of crystallization.

All atoms are located on the general *Wyckoff* position *8f* of the monoclinic space group *I2/a* (No. 15). As there is no indication for the presence of deprotonated ammonia molecules, the charge of the Sn_4 cluster sums up to -4 . The tin cluster does not show direct contacts to lithium cations as all of these are coordinated by four ammonia molecules which results in tetrahedrally shaped $[\text{Li}(\text{NH}_3)_4]^+$ complexes that can be considered as large and approximately spherical cationic units (Figure 6). For details, see Section 4.2. The ammonia lithium distances of 2.064(1)–2.116(1) Å in the tetrahedral cationic complex $[\text{Li}(\text{NH}_3)_4]^+$ are in good agreement with literature-known lithiumtetraammine complexes [38]. The $[\text{Sn}_4]^{4-}$ cage is coordinated by eight $[\text{Li}(\text{NH}_3)_4]^+$ complexes, which span vertices and faces of the cluster (Figure 6a). The distances within the tetrahedron vary between 2.9277(8)–2.9417(8) Å and lie within the expected values for $[\text{Sn}_4]^{4-}$ anions in ammoniate crystal structures. The Sn-Sn-Sn angles range between 59.882(20)° and 60.276(20)°.

3.6. $\text{K}_{4.5}\text{Sn}_4(\text{OH})_{0.5}\cdot 1.75\text{NH}_3$

Red, prismatic crystals of the composition $\text{K}_{4.5}\text{Sn}_4(\text{OH})_{0.5}\cdot 1.75\text{NH}_3$ could be synthesized by dissolving elemental tin with stoichiometric amounts of potassium in the presence of *t*BuOH in liquid ammonia. The hydroxide in the solvate structure is probably formed due to impurities on the potassium. The asymmetric unit of the solvate structure consists of four tetrastannide tetraanions, two hydroxide ions and seven ammonia molecules of crystallization. They all occupy general *Wyckoff* positions of the monoclinic space group *P2₁/c* (No. 14). The bond lengths of the tetrastannides of 2.884(2)–2.963(2) Å are within the expected values for Sn-Sn distances in tin tetrahydrides [30]. Three of the four crystallographically independent tin anions are coordinated by 14 potassium cations, the fourth anion is coordinated by 16 cations at distances between 3.438(5) Å and 3.145(5) Å (Figure 7a,b). The cations coordinate vertex tin atoms or span edges and faces of the tetrahedra.

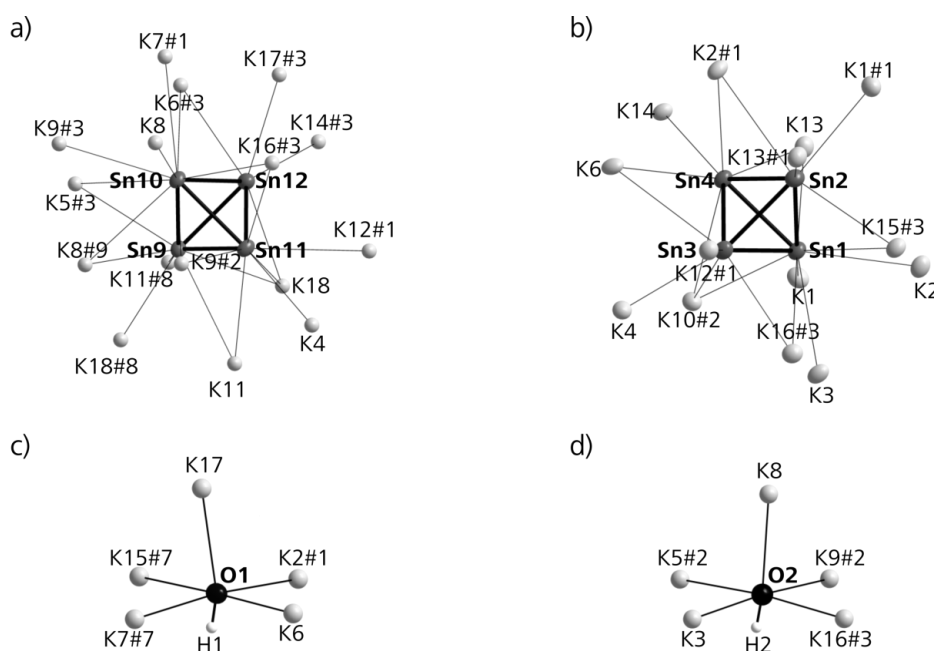


Figure 7. Cationic coordination spheres of the two anionic components in $\text{K}_{4.5}\text{Sn}_4(\text{OH})_{0.5}\cdot 1.75\text{NH}_3$; (a) $[\text{Sn}_4]^{4-}$ surrounded by 16 cations; (b) $[\text{Sn}_4]^{4-}$ coordinated by 14 cations, as a representative for the other two crystallographically independent $[\text{Sn}_4]^{4-}$ cages in the asymmetric unit; (c,d) cationic environment of the two hydroxide anions; probability factor: 50%.

Figure 7 additionally shows the coordination sphere of the second anionic component of the solvate structure, the hydroxide anions. They are characteristically surrounded by five potassium cations in a distorted square pyramidal manner. The coordination sphere of the cations is completed

by tin clusters, hydroxide ions or/and ammonia molecules of crystallization (Figure 7c,d). Altogether, the structure of $K_{4.5}Sn_4(OH)_{0.5} \cdot 1.75NH_3$ consists of strands of ammonia molecules, hydroxide anions and potassium cations, which are connected via tetrastannide anions.

4. Discussion

In this section we discuss similarities and differences of the binary compounds towards the solvate structures with respect to the coordination spheres of the cations and the cluster anions.

4.1. NaPb Type Analogies

As already mentioned in the introduction, all alkali metal stannides and plumbides with the nominal composition AE, except the compounds containing lithium, crystallize in the tetragonal space group $I4_1/acd$ (No. 142) and belong to the NaPb structure type [10,18–21]. Considering the direct cationic environment of the tetrelide cluster in the binary phase (Figure 2c), the coordination number (CN) sums up to 16. With increasing content of ammonia molecules of crystallization, the coordination number of the cages decrease (Table 4). Figure 2 shows which cation-anion contacts are broken within the solvate structures. Generally, there are three different modes of the coordination of the cation towards the anion (Figure 8).

In the binary phases and $Na_4Sn_4 \cdot 13NH_3$ [31,32] all triangular faces of the anions are capped η^3 -like by cations. In contrast, in $A_4E_4 \cdot 2NH_3$ ($A = K, Rb; E = Sn, Pb$) [30] three faces and in $Cs_4Pb_4 \cdot 5NH_3$ only one face of the $[E_4]^{4-}$ anions are coordinated η^3 -like by the cations. In addition to the coordination of the faces, the edges of the $[E_4]^{4-}$ tetrahedra are coordinated η^2 -like. For NaPb, $Rb_4Sn_4 \cdot 2NH_3$, $Cs_4Sn_4 \cdot 2NH_3$ and $Rb_4Pb_4 \cdot 2NH_3$, four η^2 -like coordinated cations are present. In $Cs_4Pb_4 \cdot 5NH_3$ five cations coordinate to the cage in a η^2 -like fashion, in $Na_4Sn_4 \cdot 11.5NH_3$ only two. Finally, the cationic environment of the $[E_4]^{4-}$ anions in the binary phase is completed by a total of eight cations which are bonded η^1 -like to each vertex. In $Rb_4Sn_4 \cdot 2NH_3$, $Cs_4Sn_4 \cdot 2NH_3$, $Rb_4Pb_4 \cdot 2NH_3$ and $Cs_4Pb_4 \cdot 5NH_3$ three and two vertices are coordinated by two cations, respectively. The other vertices each only show one tetrelide-alkali metal contact. Table 4 summarizes the anion coordinations and it becomes evident that the solvate structures with a small content of ammonia molecules of crystallization are more similar to the solid state structure, thus the three-dimensional cation-anion interactions are considerably less disturbed. Additionally, more anion-cation contacts appear in the solvate structures with the heavier alkali metals. Rubidium and cesium, as well as tin and lead are considered as soft acids and bases according to the HSAB theory [50]. The solvate structures containing sodium show much less anion-cation contacts due to the favored interaction of the hard base ammonia to the hard acid sodium cation (Table 5). Table 5 additionally shows the total coordination numbers of the cations, which is classified into cation-anion ($A^+ - E^-$) and cation-nitrogen ($A^+ - NH_3$) contacts. In $Na_4Sn_4 \cdot 13NH_3$, $Na_4Sn_4 \cdot 11.5NH_3$ and $Cs_4Pb_4 \cdot 5NH_3$ the numbers of anion-cation contacts and the cation-nitrogen contacts are similar. In contrast, $Rb_4Sn_4 \cdot 2NH_3$, $Cs_4Sn_4 \cdot 2NH_3$ and $Rb_4Pb_4 \cdot 2NH_3$ show more $A^+ - E^-$ contacts than ion-dipole interactions between the cation and the ammonia molecules of crystallization.

Table 4. Coordination number of the $[E_4]^{4-}$ cages in NaPb and related compounds.

Compound	Coordination Number (CN) $E^- - A^+$	η^1 -like Coordination	η^2 -like Coordination	η^3 -like Coordination
NaPb Type	16	8	4	4
$Na_4Sn_4 \cdot 13NH_3$	4	/	/	4
$Na_4Sn_4 \cdot 11.5NH_3$	5	/	2	3
$Cs_4Pb_4 \cdot 5NH_3$	12	6	5	1
$Rb_4Sn_4 \cdot 2NH_3 / Cs_4Sn_4 \cdot 2NH_3 / Rb_4Pb_4 \cdot 2NH_3$	14	7	4	3

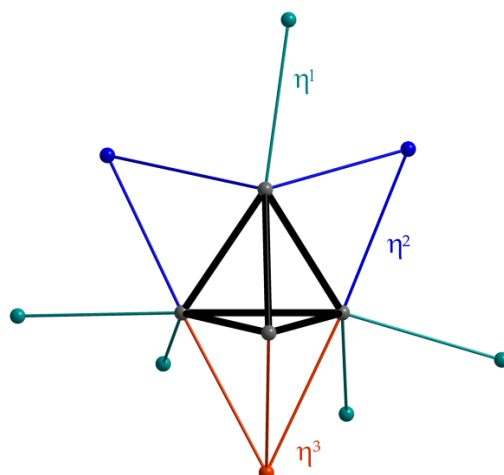


Figure 8. Different coordination modes of cations shown on the example of NaPb.

Table 5. Coordination number of the cations in NaPb and related ammoniates.

Compound	CN _{total} of Cations	A ⁺ -E ⁻ Contacts	A ⁺ -NH ₃ Contacts
NaPb Type	6–8	6–8	0
Na ₄ Sn ₄ ·13NH ₃	7	3	4
Na ₄ Sn ₄ ·11.5NH ₃	5–6	2–3	0–3
Cs ₄ Pb ₄ ·5NH ₃	9–10	4–5	4–6
Rb ₄ Sn ₄ ·2NH ₃ /Cs ₄ Sn ₄ ·2NH ₃ /Rb ₄ Pb ₄ ·2NH ₃	8–11	5–7	2–4

4.2. KGe Type Analogies

Binary alkali metal compounds of silicon and germanium with the nominal composition AB (A = K–Cs) crystallize in the KGe structure type (Figure 5, for the corresponding literature see Table 1) [11–17]. Table 6 shows the number of cations coordinated to the [E₄]⁴⁻ cages. Here again, the decrease of the CN is directly related to the content of ammonia in the solvate structure. Like in the NaPb structure type, four cations coordinate η³-like to all triangular faces of the cages. However, unlike the NaPb type, no η²-like bonded cations are present in this solid state structure. Here, only single cation-anion contacts between the vertex atoms and the cations are built. The CN sums up to 16. The cationic environment of the [E₄]⁴⁻ clusters of the compounds Cs₄Ge₄·9NH₃ and [Li(NH₃)₄]₄Sn₄·4NH₃ is very similar to those of the KGe structure. It consists of four η³-like bonded cations/cationic complexes that are situated on the faces of the cages. However, in these ammoniates, every vertex is only coordinated by one cation/cationic complex instead of three. Thus, the CN has a value of eight for the anionic clusters in Cs₄Ge₄·9NH₃ and [Li(NH₃)₄]₄Sn₄·4NH₃ (Table 6). The situation for the [Si₄]⁴⁻ tetrahedra in Cs₄Si₄·7NH₃ looks a bit different. Here also four cations which span the triangular faces of the cages are found next to three (for Si₄ (1)) and four (for Si₄ (2)) η¹-like bonded cations, respectively (Figure 5a,b). The coordination spheres of the cages are completed by two and three cations, respectively, which coordinate to edges (η²-like) of the cages. This kind of coordination is more prevalent in the NaPb structure type (Figure 2). The CN of the [Si₄]⁴⁻ cages sums up to 9/11 (Table 6).

Cs ammoniates of all group 14 elements are now known (Cs₄Si₄·7NH₃, Cs₄Ge₄·9NH₃, Cs₄Sn₄·2NH₃ and Cs₄Pb₄·5NH₃), which allows for comparison of the coordination number of the Cs cation. As mentioned in the introduction, the [E₄]⁴⁻ cages can be considered as roughly spherical with a radius calculated from the distance of the center of the tetrahedron to the edges (averaged distances) plus the *van der Waals* radius of the particular element [25]. Naturally, the sizes of the silicide (radius *r*: 3.58 Å) and the germanide (*r*: 3.67 Å) clusters are smaller than those of the stannide (*r*: 3.96 Å) and plumbide (*r*: 3.90 Å) clusters. This affects the CN of the cation. As listed in Tables 5 and 7, which show

the coordination number of the cations in NaPb/KGe and the related ammoniates, the CN of Cs⁺ amounts to 9–11 in Cs₄Pb₄·5NH₃ and Cs₄Sn₄·2NH₃. In Cs₄Si₄·7NH₃ and Cs₄Ge₄·9NH₃ the CN sums up to 10–13 and thus is significantly higher. In addition, the total coordination number consists of the cation-anion (A⁺-E⁻) and the cation-nitrogen contacts (A⁺-NH₃). Considering the A⁺-E⁻ contacts in Cs₄Si₄·7NH₃ and Cs₄Ge₄·9NH₃, remarkably fewer (2–7) can be found in comparison to the ion-dipole interactions (4–9) between the cesium cations and the ammonia molecules of crystallization. In contrast, in Cs₄Pb₄·5NH₃ and Cs₄Sn₄·2NH₃ more A⁺-E⁻ contacts (4–7) than A⁺-NH₃ (2–6) interactions occur. The reduced cation-NH₃ contacts in the solvate structures of the heavier homologues tin and lead indicates that the size of the clusters has a significant impact on the quantity of ammonia molecules of crystallization that coordinate to the cesium cation and thus complete the coordination sphere.

Altogether, it is shown that the content of ammonia molecules of crystallization directly correlates with the CN of the cages to cations (see Section 4.1). This means that the presence of ammonia molecules results in broken anion-cation contacts within the ionic framework.

Table 6. Coordination number of the [E₄]⁴⁻ cages in KGe and related ammoniates.

Compound	Coordination Number (CN) E ⁻ -A ⁺	η ¹ -like Coordination	η ² -like Coordination	η ³ -like Coordination
KGe Type	16	12	/	4
Cs ₄ Si ₄ ·7NH ₃	9/11	3/4	2/3	4/4
Cs ₄ Ge ₄ ·9NH ₃	8	4	/	4
[Li(NH ₃) ₄] ₄ Sn ₄ ·4NH ₃	8	4	/	4

Table 7. Coordination number of the cations in KGe and related ammoniates.

Compound	CN _{total} of Cations	A ⁺ -E ⁻ Contacts	A ⁺ -NH ₃ Contacts
KGe Type	6	6	0
Cs ₄ Si ₄ ·7NH ₃	10–13	2–7	4–9
Cs ₄ Ge ₄ ·9NH ₃	13	4	9
[Li(NH ₃) ₄] ₄ Sn ₄ ·4NH ₃	7	3	4

4.3. Effect of Additional Anions within Solvate Structures

In K_{4.5}Sn₄(OH)_{0.5}·1.75NH₃, the cationic environment slightly differs from the binary system NaPb and from the other solvate structures due to the presence of another anionic component, the hydroxide anion. As already mentioned in Section 3.6, the asymmetric unit consists of four crystallographically independent [Sn₄]⁴⁻ clusters. The coordination number of three of them has a value of 14, the CN of the fourth cluster is 16. Although ammonia molecules of crystallization are present in the structure, the CN of the clusters are very similar to the CN of the binary solid state system or are rather insignificantly smaller. Mainly, the differences lie in the manner of the coordination of the cations to the cages. In K_{4.5}Sn₄(OH)_{0.5}·1.75NH₃, only one to two (for Sn₄ (2)) cations span triangular faces of the cage, compared to the binary phase and the other solvate structures described in Section 4.1, where four and three cations coordinate in a η³-like fashion. The number of the η²-like bonded cations is somewhat higher. They can be found five or rather six times. The remaining cationic environment of the stannide clusters is built up by six to nine cations, which are η¹-like attached to vertex tin atoms. In the binary system, every vertex atom of the cluster shows two single cation-anion contacts, so eight η¹-like bonded cations appear here. Altogether, the presence of another anionic component and ammonia molecules of crystallization lead to different cationic coordinations of the anionic cages compared to the other solvate structures. But taking the slight content of ammonia molecules and hydroxide anion per stannide cluster into account, it is not surprising that the number of coordinating cations is almost equal to that in the binary phase NaPb.

5. Conclusions

We investigated the relations of ammoniate crystal structures of tetrelide tetrahydrides and the corresponding binary intermetallic phases. The involvement of ammonia strongly influences the structures of the compounds due to its character of rather acting as ligand towards the alkali metal cations than as an innocent solvent molecule. This is reflected in the CN of the cations as well as the anions. For the small alkali metal cations of lithium and sodium (hard acids) this even results in a formal enlargement of the cation radius which finally ends up in the structural similarities especially for Li-ammonia containing compounds to the binaries of the heavier homologues. Additional charged anions within the solvate crystal structures influence the overall crystal structure and this leads to a different cationic coordination of the anionic cages compared to the other solvate structures.

Author Contributions: C.L. and S.G. carried out experimental work (synthesis, crystallization, X-ray structure determination), C.L. and S.G. prepared the manuscript, N.K. designed and conceived the study.

Funding: This research received no external funding.

Conflicts of Interest: The authors declare no conflict of interest.

Appendix A

Appendix A.1 Experimental Details

All operations were carried out under argon atmosphere using standard Schlenk and Glovebox techniques. Liquid ammonia was dried and stored on sodium in a dry ice cooled Dewar vessel for at least 48 h. Silicon (powder, 99%, 2N+, ABCR) and Lithium (99%, Chemmetal, Langelshiem) was used without further purification. Sodium (>98%, Merck, Deutschland) and potassium (>98%, Merck, Deutschland) were purified by liquating. Rubidium and cesium were synthesized according to Hackspill [51] and distilled for purification. [18]crown-6 was sublimated under dynamic vacuum at 353 K. [2.2.2]cryptand (ABCR) was used without further purification. In the reaction mixtures containing the two chelating agents, crystals of the composition $C_{12}H_{24}O_6 \cdot 2NH_3$ [52] and $C_{18}H_{36}O_6N_2 \cdot 2NH_3$ [52] could additionally be observed. For the reaction mixtures with $tBuOH$, surprisingly no crystal structures containing $tBuOH$ or $tBuO^-$ could be found.

Appendix A.1.1 Direct Reduction

$[Li(NH_3)_4]_4Sn_4 \cdot 4NH_3$, $Na_4Sn_4 \cdot 11.5NH_3$, $K_{4.5}Sn_4(OH)_{0.5} \cdot 1.75NH_3$ and $Cs_4Pb_4 \cdot 5NH_3$: Tin and lead, respectively, as well as the stoichiometric amount of alkali metals, were placed in a three times baked out Schlenk vessel in a glovebox under argon atmosphere. For the synthesis of $[Li(NH_3)_4]_4Sn_4 \cdot 4NH_3$, $Na_4Sn_4 \cdot 11.5NH_3$ and $K_{4.5}Sn_4(OH)_{0.5} \cdot 1.75NH_3$ $tBuOH$ was additionally placed in the Schlenk vessel (the difference in applied amount of alkali metal and crystallized stoichiometry is explainable due to traces of water in $tBuOH$ despite intensive drying). About 10 mL of dry liquid ammonia was condensed on the mixture at 195 K. The appropriate amount of $tBuOH$ was added by a syringe at 195 K under immediate freezing. The blue ammonia alkali metal solution was allowed to react with $tBuOH$ and tin at 236 K. Gassing was observed first and the color of the solution changed from blue to dark red within few days. After storage at 236 K for a few weeks crystals of the above discussed compounds could be obtained.

$[Li(NH_3)_4]_4Sn_4 \cdot 4NH_3$: 0.3 g Sn (2.6 mmol), 0.0905 g Li (13.1 mmol) and 1 mL $tBuOH$ (0.77 g, 10.4 mmol).

$Na_4Sn_4 \cdot 11.5NH_3$: 0.95 g Sn (8.0 mmol), 0.4 g Na (17.4 mmol) and 1 mL $tBuOH$ (0.77 g, 10.4 mmol).

For N6, a split position was introduced as well as a SIMU restraint.

$K_{4.5}Sn_4(OH)_{0.5} \cdot 1.75NH_3$: 0.475 g Sn (4.0 mmol), 0.340 g K (8.7 mmol) and 0.5 mL $tBuOH$ (0.385 g, 5.2 mmol).

$Cs_4Pb_4 \cdot 5NH_3$: 0.1729 g Pb (0.835 mmol), 0.1109 g Cs (0.835 mmol).

Appendix A.1.2 Solvolysis

Synthesis of the precursor $\text{Cs}_{12}\text{Si}_{17}$ and $\text{Cs}_{12}\text{Ge}_{17}$: For $\text{Cs}_{12}\text{Si}_{17}$, Cs (1.539 g, 11.581 mmol) and Si (0.461 g, 16.407 mmol), for $\text{Cs}_{12}\text{Ge}_{17}$, Cs (1.127 g, 8.481 mmol) and Ge (0.873 g, 12.015 mmol) were enclosed in tantalum containers and jacketed in an evacuated ampoule of fused silica. The containers were heated to 1223 K at a rate of $25 \text{ K}\cdot\text{h}^{-1}$. The temperature was kept for 2 h. The ampoule was cooled down with a rate of $20 \text{ K}\cdot\text{h}^{-1}$. The precursors were stored in a glove box under argon.

$\text{Cs}_4\text{Si}_4\cdot 7\text{NH}_3$ and $\text{Cs}_4\text{Ge}_4\cdot 9\text{NH}_3$: 50 mg of each precursor were dissolved in about 15 ml of liquid ammonia together with two chelating agents, [18]crown-6/dicyclohexano[18]crown-6 and [2.2.2]cryptand. The rufous solutions were stored at 197 K. After several months, very few crystals of the above discussed compounds could be obtained.

$\text{Cs}_4\text{Si}_4\cdot 7\text{NH}_3$: 50 mg (0.0245 mmol) of $\text{Cs}_{12}\text{Si}_{17}$, 9.4 mg (0.0252 mmol) dicyclohexano[18]crown-6 and 18.5 mg (0.0491 mmol) [2.2.2]cryptand. For Cs5 a split position was introduced and a SIMU restraint was applied.

$\text{Cs}_4\text{Ge}_4\cdot 9\text{NH}_3$: 50 mg (0.025 mmol) of $\text{Cs}_{12}\text{Ge}_{17}$, 0.0513 mg (0.194 mmol) [18]crown-6 and 0.044 mg (0.116 mmol) [2.2.2]cryptand. To prevent N2 and N3 to go non-positive definite (N.P.D.), the two atoms were refined isotropically and the atom radii were fixed at 0.05.

References

1. Korber, N. Metal Anions: Defining the Zintl Border. *Z. Anorg. Allg. Chem.* **2012**, *638*, 1057–1060. [[CrossRef](#)]
2. Nesper, R. The Zintl-Klemm Concept—A Historical Survey. *Z. Anorg. Allg. Chem.* **2014**, *640*, 2639–2648. [[CrossRef](#)]
3. Dubois, J.M.E.; Belin-Ferre, E.E. *Complex Metallic Alloys: Fundamentals and Applications*; Wiley-VCH Verlag GmbH: Weinheim, Germany, 2011.
4. Westbrook, J.H.; Fleischer, R.L. *Intermetallic Compounds, Principles and Practice*; Wiley: New York, NY, USA, 2002; Volume 3.
5. Guloy, A.M. Polar Intermetallics and Zintl Phases along the Zintl Border. In *Inorganic Chemistry in Focus III*; Wiley-VCH Verlag GmbH & Co. KGaA: Weinheim, Germany, 2006.
6. Zintl, E. Intermetallische Verbindungen. *Angew. Chem.* **1939**, *52*, 1–6. [[CrossRef](#)]
7. Klemm, W. Metalloids and their compounds with the alkali metal. *Proc. Chem. Soc. Lond.* **1958**, *12*, 329–341.
8. Gärtner, S.; Korber, N.; Poepelmeier, K.E.; Reedijk, J.E. *Main-Group Elements, Comprehensive Inorganic Chemistry II*, 2nd ed.; Elsevier Ltd.: Amsterdam, The Netherlands, 2013; Volume 140.
9. Fässler, T.F. *Structure and Bonding*; Springer: Berlin/Heidelberg, Germany, 2011; Volume 140.
10. Marsh, R.E.; Shoemaker, D.P. The crystal structure of NaPb. *Acta Cryst.* **1953**, *6*, 197–205. [[CrossRef](#)]
11. Busmann, E. Das Verhalten der Alkalimetalle zu Halbmetallen. X. Die Kristallstrukturen von KSi, RbSi, CsSi, KGe, RbGe und CsGe. *Z. Anorg. Allg. Chem.* **1961**, *313*, 90–106. [[CrossRef](#)]
12. Von Schnering, H.G.; Schwarz, M.; Chang, J.-H.; Peters, K.; Peters, E.-M.; Nesper, R. Refinement of the crystal structures of the tetrahedrotetrasilicides K_4Si_4 , Rb_4Si_4 and Cs_4Si_4 . *Z. Kristallogr. NCS* **2005**, *220*, 525–527. [[CrossRef](#)]
13. Von Schnering, H.G.; Llanos, J.; Chang, J.H.; Peters, K.; Peters, E.M.; Nesper, R. Refinement of the crystal structures of the tetrahedro-tetragermanides K_4Ge_4 , Rb_4Ge_4 and Cs_4Ge_4 . *Z. Kristallogr. NCS* **2005**, *220*, 324–326. [[CrossRef](#)]
14. Schäfer, R.; Klemm, W. Das Verhalten der Alkalimetalle zu Halbmetallen. IX. Weitere Beiträge zur Kenntnis der Silicide und Germanide der Alkalimetalle. *Z. Anorg. Allg. Chem.* **1961**, *312*, 214–220. [[CrossRef](#)]
15. Hohmann, E. Silicide und Germanide der Alkalimetalle. *Z. Anorg. Allg. Chem.* **1948**, *257*, 113–126. [[CrossRef](#)]
16. Witte, J.; von Schnering, H.G. Die Kristallstruktur von NaSi und NaGe. *Z. Anorg. Allg. Chem.* **1964**, *327*, 260. [[CrossRef](#)]
17. Goebel, T.; Ormeci, A.; Pecher, O.; Haarmann, F. The Silicides M_4Si_4 with M = Na, K, Rb, Cs, and Ba_2Si_4 —NMR Spectroscopy and Quantum Mechanical Calculations. *Z. Anorg. Allg. Chem.* **2012**, *638*, 1437–1445. [[CrossRef](#)]
18. Baitinger, M.; Grin, Y.; von Schnering, H.G.; Kniep, R. Crystal structure Rb_4Sn_4 and Cs_4Sn_4 . *Z. Kristallogr. New Cryst. Struct.* **1999**, *214*, 457–458.

19. Grin, Y.; Baitinger, M.; Kniep, R.; von Schnering, H.G. Redetermination of the crystal structure of tetrasodium tetrahedrotetastannide, Na_4Sn_4 and tetrapotassium tetrahedro-tetastannide, K_4Sn_4 . *Z. Kristallogr New Cryst. Struct.* **1999**, *214*, 453–454. [[CrossRef](#)]
20. Baitinger, M.; Peters, K.; Somer, M.; Carrillo-Cabrera, W.; Grin, Y.; Kniep, R.; von Schnering, H.G. Crystal structure of tetrarubidium tetrahedro-tetraplumbide, Rb_4Pb_4 and of tetracaesium tetrahedro-tetraplumbide, Cs_4Pb_4 . *Z. Kristallogr. NCS* **1999**, *214*, 455–456.
21. Hewaidy, I.F.; Busmann, E.; Klemm, W. Die Struktur der AB-Verbindungen der schweren Alkalimetalle mit Zinn und Blei. *Z. Anorg. Allg. Chem.* **1964**, *328*, 283–293. [[CrossRef](#)]
22. Goebel, T.; Prots, Y.; Haarmann, F. Refinement of the crystal structure of tetrasodium tetrasilicide, Na_4Si_4 . *Z. Kristallogr. NCS* **2008**, *223*, 187–188. [[CrossRef](#)]
23. Evers, J.; Oehlinger, G.; SEXTL, G. LiSi, a Unique Zintl Phase—Although Stable, It Long Evaded Synthesis. *Eur. J. Solid State Inorg. Chem.* **1997**, *34*, 773–784.
24. Menges, E.; Hopf, V.; Schaefer, H.; Weiss, A. Die Kristallstruktur von LiGe—ein neuartiger, dreidimensionaler Verband von Element (IV)-atomen. *Z. Naturf. B.* **1969**, *24*, 1351–1352. [[CrossRef](#)]
25. Holleman, A.F.; Wiberg, E.; Wiberg, N. *Anorganische Chemie*, 103rd ed.; Walter de Gruyter GmbH: Berlin, Germany, 2017.
26. Müller, W.; Schäfer, H. Crystal-structure of LiSn. *Z. Naturforsch. B* **1973**, *B 28*, 246–248.
27. Müller, W.; Volk, K. Die Struktur des beta-NaSn. *Z. Naturforsch.* **1977**, *B 32*, 709–710.
28. Nowotny, H. The structure of LiPb. *Z. Metallkunde* **1941**, *33*, 388.
29. Neumeier, M.; Fendt, F.; Gaertner, S.; Koch, C.; Gaertner, T.; Korber, N.; Gschwind, R.M. Detection of the Elusive Highly Charged Zintl Ions $[\text{Si}_4]^{4-}$ and $[\text{Sn}_4]^{4-}$ in Liquid Ammonia by NMR Spectroscopy. *Angew. Chem. Int. Ed.* **2013**, *52*, 4483–4486. [[CrossRef](#)] [[PubMed](#)]
30. Wiesler, K.; Brandl, K.; Fleischmann, A.; Korber, N. Tetrahedral $[\text{Tt}_4]^{4-}$ Zintl Anions through Solution Chemistry: Syntheses and Crystal Structures of the Ammoniates $\text{Rb}_4\text{Sn}_4 \cdot 2\text{NH}_3$, $\text{Cs}_4\text{Sn}_4 \cdot 2\text{NH}_3$, and $\text{Rb}_4\text{Pb}_4 \cdot 2\text{NH}_3$. *Z. Anorg. Allg. Chem.* **2009**, *635*, 508–512. [[CrossRef](#)]
31. Fleischmann, A. Synthese und Strukturelle Charakterisierung homoatomarer Polyanionen der vierten und fünften Hauptgruppe durch Reduktion in flüssigem Ammoniak. Ph.D. Thesis, University of Regensburg, Regensburg, Germany, 2002.
32. Waibel, M.; Fässler, T.F. First Incorporation of the Tetrahedral $[\text{Sn}_4]^{4-}$ Cluster into a Discrete Solvate $\text{Na}_4[\text{Sn}_4](\text{NH}_3)_{13}$ from Solutions of Na_4Sn_4 in Liquid Ammonia. *Z. Naturforsch. B* **2013**, *68*, 732–734. [[CrossRef](#)]
33. Lorenz, C.; Gärtner, S.; Korber, N. $[\text{Si}_4]^{4-}$ in Solution—First Solvate Crystal Structure of the Ligand-free Tetrasilicide Tetraanion in $\text{Rb}_{1.2}\text{K}_{2.8}\text{Si}_4 \cdot 7\text{NH}_3$. *Z. Anorg. Allg. Chem.* **2017**, *643*, 141–145. [[CrossRef](#)]
34. Fendt, F. Untersuchungen zum Lösungs- und Reaktionsverhalten von Polystanniden und -siliciden in flüssigem Ammoniak. Ph.D. Thesis, University of Regensburg, Regensburg, Germany, 2016.
35. Joseph, S.; Suchentrunk, C.; Kraus, F.; Korber, N. $[\text{Si}_9]^{4-}$ Anions in Solution—Structures of the Solvates $\text{Rb}_4\text{Si}_9 \cdot 4.75 \text{NH}_3$ and $[\text{Rb} (18\text{-crown-6})] \text{Rb}_3\text{Si}_9 \cdot 4\text{NH}_3$, and Chemical Bonding in $[\text{Si}_9]^{4-}$. *Eur. J. Inorg. Chem.* **2009**, *2009*, 4641–4647. [[CrossRef](#)]
36. Joseph, S.; Suchentrunk, C.; Korber, N. Dissolving Silicides: Syntheses and Crystal Structures of New Ammoniates Containing Si_5^{2-} and Si_9^{4-} Polyanions and the Role of Ammonia of Crystallisation. *Z. Naturforsch.* **2010**, *B65*, 1059–1065. [[CrossRef](#)]
37. Suchentrunk, C.; Daniels, J.; Somer, M.; Carrillo-Cabrera, W.; Korber, N. Synthesis and Crystal Structures of the Polygermanide Ammoniates $\text{K}_4\text{Ge}_9 \cdot 9 \text{NH}_3$, $\text{Rb}_4\text{Ge}_9 \cdot 5 \text{NH}_3$ And $\text{Cs}_6\text{Ge}_{18} \cdot 4 \text{NH}_3$. *Z. Naturforsch.* **2005**, *B60*, 277–283.
38. Korber, N.; Fleischmann, A. Synthesis and crystal structure of $[\text{Li}(\text{NH}_3)_4]_4[\text{Sn}_9] \cdot \text{NH}_3$ and $[\text{Li}(\text{NH}_3)_4]_4[\text{Pb}_9] \cdot \text{NH}_3$. *Dalton Trans.* **2001**, *4*, 383–385. [[CrossRef](#)]
39. Carrillo-Cabrera, W.; Aydemir, U.; Somer, M.; Kircali, A.; Fassler, T.F.; Hoffmann, S.D. Cs_4Ge_9 -en: A Novel Compound with $[\text{Ge}_9]^{4-}$ Clusters—Synthesis, Crystal Structure and Vibrational Spectra. *Z. Anorg. Allg. Chem.* **2007**, *633*, 1575–1580. [[CrossRef](#)]
40. Somer, M.; Carrillo-Cabrera, W.; Peters, E.M.; Peters, K.; von Schnering, H.G. Tetrarubidium Nonagermanide (4-) Ethylenediamine, $\text{Rb}_4[\text{Ge}_9][\text{en}]$. *Z. Anorg. Allg. Chem.* **1998**, *624*, 1915–1921. [[CrossRef](#)]
41. Edwards, P.A.; Corbett, J.D. Stable homopolyatomic anions. Synthesis and crystal structures of salts containing the pentaplumbide (2-) and pentastannide (2-) anions. *Inorg. Chem.* **1977**, *16*, 903–907. [[CrossRef](#)]

42. Goicoechea, J.M.; Sevov, S.C. Naked Deltahedral Silicon Clusters in Solution: Synthesis and Characterization of Si_9^{3-} and Si_5^{2-} . *J. Am. Chem. Soc.* **2004**, *126*, 6860–6861. [[CrossRef](#)] [[PubMed](#)]
43. Suchentrunk, C.; Korber, N. Ge_5^{2-} Zintl anions: synthesis and crystal structures of $[\text{K}([2.2.2]\text{-crypt})]_2\text{Ge}_5\cdot 4\text{NH}_3$ and $[\text{Rb}([2.2.2]\text{-crypt})]_2\text{Ge}_5\cdot 4\text{NH}_3$. *New J. Chem.* **2006**, *30*, 1737–1739. [[CrossRef](#)]
44. Friedrich, U.; Korber, N. $\text{Cs}_5\text{Sn}_9(\text{OH})\cdot 4\text{NH}_3$. *Acta Crystallogr. E* **2014**, *70*, i29. [[CrossRef](#)] [[PubMed](#)]
45. Kottke, T.; Stalke, D. Crystal handling at low temperatures. *J. Appl. Crystallogr.* **1993**, *26*, 615–619. [[CrossRef](#)]
46. Stalke, D. Cryo crystal structure determination and application to intermediates. *Chem. Soc. Rev.* **1998**, *27*, 171–178. [[CrossRef](#)]
47. Rigaku. *Crystalis pro, Version 1.171.38.46*; Agilent Technologies: Santa Clara, CA, USA, 2017.
48. X-RED. *STOE & Cie GmbH Darmstadt 1998*; X-RED Data Reduction for STADI4 and IPDS: Darmstadt, Germany, 1998.
49. Fendt, F.; Koch, C.; Gartner, S.; Korber, N. Reaction of Sn_4^{4-} in liquid ammonia: the formation of $\text{Rb}_6[(\eta^2\text{-Sn}_4)\text{Zn}(\eta^3\text{-Sn}_4)]\cdot 5\text{NH}_3$. *Dalton Trans.* **2013**, *42*, 15548–15550. [[CrossRef](#)] [[PubMed](#)]
50. Pearson, R.G. Hard and Soft Acids and Bases. *J. Am. Chem. Soc.* **1963**, *85*, 3533–3539. [[CrossRef](#)]
51. Hackspill, L. Some properties of the alkali metals. *Helv. Chim. Acta* **1928**, *11*, 1.
52. Suchentrunk, C.; Rossmier, T.; Korber, N. Crystal structures of the [18]-crown-6 ammoniate $\text{C}_{12}\text{H}_{24}\text{O}_6\cdot 2\text{NH}_3$ and the cryptand [2.2.2] ammoniate $\text{C}_{18}\text{H}_{36}\text{O}_6\text{N}_2\cdot 2\text{NH}_3$. *Z. Kristallogr.* **2006**, *221*, 162–165.



© 2018 by the authors. Licensee MDPI, Basel, Switzerland. This article is an open access article distributed under the terms and conditions of the Creative Commons Attribution (CC BY) license (<http://creativecommons.org/licenses/by/4.0/>).